



Journal of Advanced Research in Fluid Mechanics and Thermal Sciences

Journal homepage:
https://semarakilmu.com.my/journals/index.php/fluid_mechanics_thermal_sciences/index
ISSN: 2289-7879



The Effect of Insulation Thickness on Heat Transfer Characteristics and Flammability in Tube Mesoscale Combustors

Evita Leninda Fahriza Ayuni¹, Andinusa Rahmandhika^{1,*}, Daryono¹, Ardi Lesmawanto², Krisna Bayu Rizkyawan¹, Ali Mokhtar¹, Achmad Fauzan Hery Soegiharto¹

¹ Department of Mechanical Engineering, Faculty of Engineering, University of Muhammadiyah Malang, Indonesia

² Department of Power Mechanical Engineering, National Formosa University, Yunlin 63201, Taiwan

ARTICLE INFO

Article history:

Received 1 November 2023

Received in revised form 29 March 2024

Accepted 12 April 2024

Available online 30 April 2024

Keywords:

Mesoscale combustor; mesh; insulation thickness; flammability; heptane

ABSTRACT

Micropower generator is a micro-scale energy source that has two main components, namely a micro/mesoscale combustor and thermophotovoltaics (TPV). The micro-scale combustor is one part that functions as a combustion chamber that produces heat in micropower plants. Heptane is used as fuel, while the combustor combustion chamber with a diameter of 3.5 mm is made from duraluminium-quartz glass tube. Combustion stability in the combustion chamber is influenced by several factors, such as temperature, geometry, and combustion chamber design. In order to maintain flame stability, mesh is added to the combustion chamber. One way to minimize heat loss in the combustion chamber is to add an insulating layer to the combustion chamber. This research aims to prove the role of adding an insulating layer in flame stability in mesoscale burners. It is necessary to add an appropriate insulating layer to minimize heat loss so that it remains stable in the mesoscale burner. This experimental test shows that the temperature distribution when adding an insulation layer with a thickness of 3 mm has a higher temperature on the outside compared to a thickness of 6 mm. Meanwhile, the temperature inside the combustor chamber with a thickness of 6 mm is superior to that with a thickness of 3 mm. The flame limit of the combustor with a mesh distance of 5 mm for liquid heptane fuel was successfully stable at an equivalent ratio of $\phi 0.97 - 1.5$ with a maximum speed of 31.7.

1. Introduction

Technological developments in all fields are increasing rapidly, enabling humans to carry out new innovations. Various types of new equipment have emerged to make things easier for workers. However, this equipment of course requires energy to operate [1]. One technology area that continues to innovate is portable technology. Nonetheless, a common problem that often happens in portable equipment is the limited power capacity, while the required power is relatively large [2]. This challenge has led to the development of small power generation technology (micro power generation), which can be packaged into a power cell/battery [3,4].

* Corresponding author.

E-mail address: andinusa@umm.ac.id

<https://doi.org/10.37934/arfmts.116.2.157171>

Micro power generator (MPG) is a micro generator that utilizes combustion heat as an energy source. Micro power generators have one important component, namely mesoscale combustion or mesoscale combustor [5]. The size of the micro combustor is categorized into two scales: micro-scale with a dimension less than 1 mm, and mesoscale with a dimension more than 1 mm [6,7].

The fuel used by the micro combustor can be either liquid or gas fuel. Burning fuel in the meso combustor converts chemical energy into heat energy, which can be used to produce electricity [6]. Micro or mesoscale combustors can serve as a source of electricity for various components of communication equipment, as well as for recharging power, and more. The micro power generation system uses hydrocarbon fuel which has a higher energy density compared to batteries. Therefore, the latest advancements in micro power generation systems are highly valuable for being a solution today [8,9].

The most important discussion in micro combustor research lies in achieving flame stability within mesoscale burners [10]. Stabilizing the flame in a micro-scale burner is quite difficult due to the limited volume of the combustion chamber, causing short reactant residence time and high heat losses [11]. Consequently, as the fuel flow increases in the mesoscale, the temperature tends to increase. To determine the characteristic conditions of fluid flow at the mesoscale, observations and (theoretical) calculations need to be carried out [12]. Observations involve the flow movements investigation, including laminar flow, transition flow and turbulent flow [13]. As for the calculations, the Reynolds number (RE) equation can be employed [14].

Liquid fuels are safer and easier in terms of storage but have challenges related to evaporation and mixing with air [15]. Various studies have been carried out to stabilize liquid fuel flames in mesoscale burners [16]. Single mesh insertion, double mesh insertion, stainless steel mesh insertion, copper mesh insertion, and the use of a thermal recirculator are efforts that have been made [3,11]. The heat recirculator succeeded in stabilizing the flame through the process of evaporating the liquid fuel inside [17].

The important role of the heat recirculator is for preheating and evaporation in order to stabilize the flame, especially in connection with the use of fuel. As has been done in previous research, namely a meso scale burner with the addition of a heat recirculator component with an inner diameter of 3.5 mm with a stainless steel heat recirculator that is resistant to high temperatures.

In another study, liquid hexane fuel was successfully stabilized in a meso scale combustor using a mesh insert and heat recirculator [11]. However, there is still a significant amount of heat that could be used for preheating the reactants, which is actually wasted with the combustion gases. To utilize this heat for preheating the reactant, a mesh insert is needed to contain the flame or flue gas [11]. Room conditions must be very carefully considered during the combustion process using a meso scale combustor because the flame is very sensitive to temperature and room airflow. If the room temperature is too low, the mesoscale combustor body will cool, causing it to burn out or reduce flame stability.

Based on the arguments that have been described, heat loss through the mesoscale combustor body due to convection heat transfer to the surroundings needs to be minimized. One effective method to reduce heat loss due to convection to the surroundings is by providing an insulator layer. This research aims to determine the impact of using an insulator layer on heat transfer characteristics and flame stability characteristics.

2. Methodology

2.1 Research Installations

The research was carried out at the Micro-combustion Laboratory of Mechanical Engineering, University of Muhammadiyah Malang.

Figure 1 shows the research installation carried out. The flow of liquid heptane fuel (C_7H_{16}) is regulated and injected into the burner using a syringe pump. Air is supplied from the compressor air tank and the discharge is controlled by an air flowmeter. A probe wire or cable with a diameter of 0.2 mm is connected to a thermocouple to measure temperature. A camera complete with a macro lens is placed on the output side (exhaust) and the side of the meso scale burner to observe and document the flame.

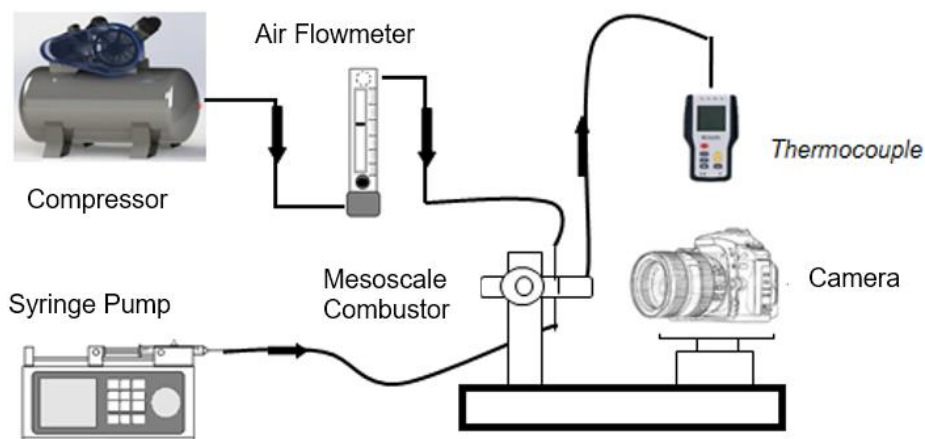


Fig. 1. Research installations

The data collection begins by applying external heating to the burner body from upstream to downstream and igniting a lighter until a flame occurs. This procedure is applied by adjusting the air and fuel discharge until a stable flame is achieved inside, after which the igniter is turned off. Flame observations were conducted for 3-5 minutes to ensure the stability of the flame. The air flow is then adjusted to obtain the minimum and maximum values. Following that, the same procedure is applied to the fuel flow, which is adjusted to obtain the minimum-maximum flow value. Again, the same procedure is carried out to determine the air discharge value, starting from the minimum to the maximum, with the flame extinguished or moved away from the flame holder.

2.2 Mesoscale Combustor

The mesoscale combustor is the main tool used in this research, in which the combustion process and flame will be observed. The body of the mesoscale burner is a duraluminium-quartz glass tube with a combustion chamber diameter of $\varnothing 3.5$ mm. A duraluminium flame holder with perforated plate lines 8 type having a thickness of 1 mm is inserted between the separator segment and the stainless steel flame retardant network. The flame holder is positioned 5 mm towards the outlet or exhaust section.

Mesoscale combustor has several parts and the size of each part has been determined as shown in Figure 2 and Figure 3: 1) Ceramic, 2) Fuel Inlet, 3) Air Inlet, 4) Heat Recirculator, 5) Annulus chamber, 6) Separator section Quartz-Glass Tube, 7) Flame Holder, 8) Flame, 9) Reaction Zone, 10) Retaining Network, 11) Quartz Glass Tube exhaust section.

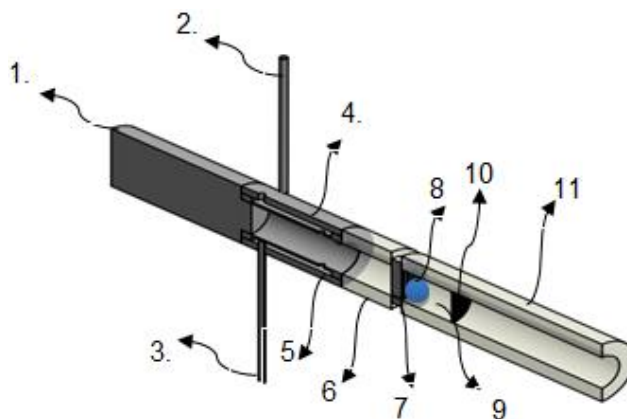


Fig. 2. Mesoscale combustor parts

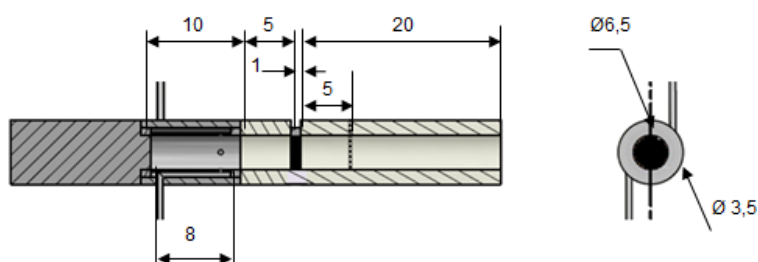


Fig. 3. Mesoscale combustor dimension

3. Results

The research data on mesoscale combustors using liquid heptane fuel with the addition of glue-based insulators were processed using Microsoft Excel. Another burner with the same design and fuel was used to compare better fuel and air mixing. Better mixing can be seen in the flame stability and heat transfer limit graphs.

There are 2 types of insulation thickness, the burner configuration with an insulation thickness of 3 mm is named type A burner. Meanwhile, the other burner configuration has an insulation thickness of 6 mm and is named burner B. Data collection is carried out by adjusting the heptane fuel discharge (Q_f) and air discharge. (Q_a) so that it approaches the stoichiometric value.

Previously, calibration was carried out to determine the actual output discharge value (Q_{actual}) on the syringe pump and air flow meter as shown in Table 1.

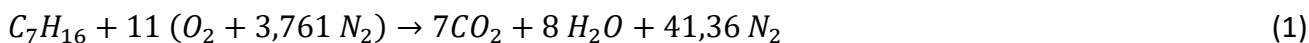
The results of flammability limit data processing are presented in the form of a flame limit graph, therefore it is necessary to know the equivalent ratio value first. The equivalent ratio (ϕ) is a comparison between the air-fuel ratio in a stoichiometric state (AFR_{stoic}) and the actual air-fuel ratio (AFR_{act}). The equivalent ratio is the flame limit of the air-fuel mixture, the flame limit is divided into two, namely the lower limit and the upper limit. The lower limit indicates that the flame is still in a stable state with constant fuel flow and maximum air flow. Meanwhile, the upper limit shows a stable flame condition with constant fuel flow and minimal air flow.

Table 1
 5 mm combustor flammability limit data

Q _{fuel} actual (ml/hr)	Q _{air} actual (ml/min)	
	min	max
0.77928	79.2152	109.1012
0.82886	79.2152	119.0632
0.87844	82.2038	128.029
0.92802	84.1962	138.9872
0.9776	89.1772	151.9378
1.02718	94.1582	158.9112
1.07676	99.1392	165.8846
1.12634	104.1202	173.8542
1.17592	112.0898	178.8352

Before calculating the value of the equivalent ratio (ϕ), it is necessary to first know the value of the air-fuel ratio in a stoichiometric state (AFR_{stoic}). Stoichiometric conditions are conditions when the air and fuel mixture has the right amount to react completely.

This research uses liquid heptane (C_7H_{16}). AFR_{stoic} air-heptane mixture with the reaction equation as shown in Eq. (1).



AFR_{stoic} is the stoichiometric air-fuel ratio obtained by dividing the air mass by the fuel mass, which can be expressed as Eq. (2).

$$\begin{aligned} AFR_{stoic} &= \frac{m_{air}}{m_{fuel}} \\ &= 15.1008 \frac{gr_{air}}{gr_{fuel}} \end{aligned} \quad (2)$$

3.1 Equivalent Ratio Calculation (ϕ)

After getting the Air Fuel Ratio value in stoichiometric conditions (AFR_{stoic}) for liquid heptane fuel, then continue calculating the equivalent ratio value (ϕ). The equivalent ratio value is obtained from the quotient of the stoichiometric air fuel ratio (AFR_{stoic}) and the actual air fuel ratio (AFR_{act}), as in the following equation:

$$\phi = \frac{AFR_{stoic}}{AFR_{act}} \quad (3)$$

where

$$AFR_{act} = \frac{\dot{m}_a}{\dot{m}_f} \quad (4)$$

Mass flow is obtained from the comparison of the densities of fuel (ρ_{fuel}) and air (ρ_{air}) with the actual flow rate of fuel (Q_f actual) and air (Q_a actual) obtained from flammability limit data. For an example of the calculation, the flammability limit data in Table 1 in the first row is taken for liquid heptane fuel on a 5 mm combustor. Heptane liquid fuel has an AFR_{stoic} value of 15.1008, Q_f actual worth 0.012988 ml/min, Q_a actual min worth 79.2152 ml/min, Q_a actual max worth 109.101 ml/min, $\rho_{heptane}$

worth 0.6838 gr/ ml, and ρ_{air} is 0.00119 gr/ml. So the flow mass (\dot{m}) of heptane fuel can be calculated using Eq. (5), Eq. (6), and Eq. (7).

$$\begin{aligned}\dot{m}_f &= \rho_{heptane} \times Q_{f actual} \\ &= 0.0088811 \text{ gr/min}\end{aligned}\quad (5)$$

$$\begin{aligned}\dot{m}_a min &= \rho_{air} \times Q_a actual min \\ &= 0.09387 \text{ gr/min}\end{aligned}\quad (6)$$

$$\begin{aligned}\dot{m}_a max &= \rho_{air} \times Q_a actual max \\ &= 0.12928 \text{ gr/min}\end{aligned}\quad (7)$$

Then, the equivalent ratio (ϕ) value for heptane fuel can be calculated using Eq. (3) and Eq. (4), thus

$$\begin{aligned}\phi_{lower limit} &= \frac{AFR_{stoic}}{\frac{\dot{m}_a max}{\dot{m}_f}} \\ &= 1.03735\end{aligned}\quad (8)$$

$$\begin{aligned}\phi_{upper limit} &= \frac{AFR_{stoic}}{\frac{\dot{m}_a min}{\dot{m}_f}} \\ &= 1.42871\end{aligned}\quad (9)$$

3.2 Calculation of Reactant Flow Velocity (U)

Calculation of the total flow velocity of reactants (U) that occurs in the combustor serves as a reference for comparison in the graph of the correlation between the equivalent ratio and the reactant velocity. Calculation of reactant velocity (U) is carried out based on the total flow rate of reactants flowing in the combustor. The use of liquid fuel is different from the use of gas fuel. Gas fuel does not have an evaporation phase because the fuel is already in gas form so it mixes more quickly with oxidants (air). Meanwhile, for liquid fuel, there is still a phase of evaporation of the fuel into gas which then mixes with air. Therefore, the fuel discharge value in the vapor phase ($Q_{f(vapor)}$) is calculated first by dividing the fuel flow mass value (\dot{m}_f) by the heptane vapor density ($\rho_{vapor heptane}$). The vapor phase density of heptane can be found using the vapor density table by knowing the boiling temperature of heptane.

It is known that the boiling temperature of heptane is 98.4 °C = 209.1 °F. Then look for the fuel vapor value ($Q_{f(vapor)}$) of heptane in the first row of data using Eq. (10).

$$\begin{aligned}Q_{f(vapor)} &= \frac{\dot{m}_f}{\rho_{vapor heptane}} \\ &= \frac{0.008881 \text{ gr/min}}{0.0033 \text{ gr/ml}} = 2.6913 \frac{\text{ml}}{\text{min}}\end{aligned}\quad (10)$$

Followed by calculating the reactant speed (U). $Q_{f(vapor)}$ is 2.6913 ml/min, $Q_a actual max$ is 109.101 ml/min, ϕ in the combustor is 3.5 mm, and radius (r) is 1.75 mm. Maximum flow rate (U_{max}) can be calculated using Eq. (11).

$$\begin{aligned}
 U_{max} &= \frac{100 \times (Q_{f(vapor)} + Q_{a \text{ actual max}})}{60 \pi r^2} \\
 &= 19.3756 \frac{cm}{s}
 \end{aligned}
 \tag{11}$$

The minimum flow rate (U_{min}) for the first data can be calculated using Eq. (12) with $Q_{f(vapor)}$ worth 2.6913 ml/min, $Q_{a \text{ actual min}}$ worth 79.2152 ml/min, ϕ in the combustor worth 3.5 mm, and radius (r) is 1.75 mm.

$$\begin{aligned}
 U_{min} &= \frac{100 \times (Q_{f(vapor)} + Q_{a \text{ actual min}})}{60 \pi r^2} \\
 &= 14.1958 \frac{cm}{s}
 \end{aligned}
 \tag{12}$$

3.3 Calculation of Reynolds Number (Re)

The Reynolds number (Re) is used to determine the distribution and value of the heat transfer coefficient [18]. By calculating the density of heptane, pipe diameter, and reactant flow velocity with air viscosity, the Reynolds Number can be obtained as shown in Eq. (13).

For an example of the calculation, the flammability limit data in Table 2 in the first row is taken for liquid heptane fuel in a 5 mm combustor. The average speed of flowing fluid (v) is 0.193756 m/s, with a diameter (D) of 0.0035 m, fluid density (ρ) of 0.0006838 kg/m³, and air viscosity (μ) of 0.000017 kg/m.s.

$$\begin{aligned}
 Re &= \frac{v \cdot D \cdot \rho}{\mu} \\
 &= 0.02728
 \end{aligned}
 \tag{13}$$

Table 2

Results of data calculations on the flammability limit of the combustor 5 mm

\dot{m}_{fuel} (gr/min)	\dot{m}_{air} (gr/min)		$Q_{f(vapor)}$ (ml/min)	ϕ Equivalent Ratio		U (cm/s)		Re
	min	max		lower	upper	min	max	
0.0088	0.093	0.129	2.6912	1.0373	1.4287	14.195	19.375	0.0272
0.0094	0.093	0.141	2.8624	1.0110	1.5196	14.225	21.131	0.0297
0.0100	0.097	0.151	3.0337	0.9964	1.5519	14.773	22.715	0.0319
0.0105	0.099	0.164	3.2049	0.9697	1.6007	15.148	24.644	0.0346
0.0111	0.105	0.180	3.3761	0.9344	1.5921	16.041	26.918	0.0378
0.0117	0.111	0.188	3.5474	0.9387	1.5843	16.934	28.156	0.0396
0.0122	0.117	0.196	3.7186	0.9427	1.5773	17.827	29.395	0.0413
0.0128	0.123	0.206	3.8898	0.9409	1.5711	18.720	30.806	0.0433
0.0134	0.132	0.211	4.0611	0.9549	1.5236	20.131	31.699	0.0446

In this research, the Reynolds number is at $Re = 0.027 - 0.044$, this value is below $Re = 2000$. This means that from the value of the Reynolds number, it can be ascertained that the type of flow is laminar. The combustor flame limit of 5 mm liquid heptane fuel was successfully stable at an equivalence ratio 0.97 – 1.5 with a maximum speed of 31.7 cm/s.

Temperature data collection was carried out to make it easier to find out how the thickness of the insulation is related to the flame on the mesoscale burner as shown in Figure 4. The addition of insulation is another factor contributing to the phenomenon of heat transfer complexity [19].

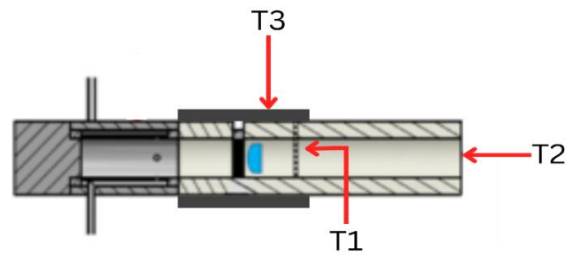


Fig. 4. Temperature intake point

The flame visualization was observed from the output (exhaust) side and the mesoscale combustor side as shown in Figure 5.

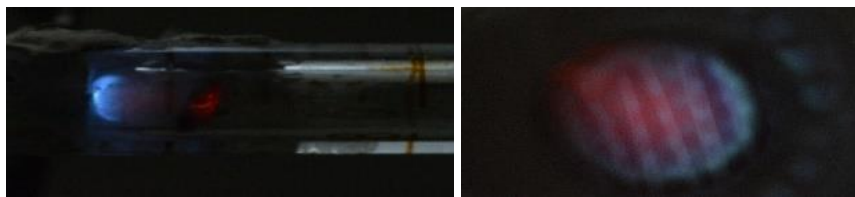


Fig. 5. Flame visualization

Table 3 and Table 4 are temperature data that have been obtained on combustors with insulation thicknesses of 3 mm and 6 mm, then plotted into graphs to make it easier to determine the temperature insulation thickness at $T3$ or the temperature of the flue gas. The correlation between reactant flow velocity and Reynolds number on temperature distribution is presented in Figure 6 and Figure 7.

Table 3

Combustor temperature data with insulation thickness of 3 mm

Reactant Flow Rate (U): 26.09 (cm/s)							
Q_{fuel}	Q_{air}	ϕ	T1	T2	T3	Flame Speed	
1	143	1.0650	251.7	101.3	196.6	22	
1.05	125	1.1153	234.4	90.6	181.5	12	
1.15	115	1.1658	247	88.1	152.9	37	
1.2	106	1.2671	250.6	74.9	155.7	67	
Constant Equivalent Ratio (ϕ): 1.25							
Q_{fuel}	Q_{air}	U (cm/s)	Reynolds Number	T1	T2	T3	Flame Speed
1	108	22.2	0.031196	234.6	80.9	160.9	71
1.05	127	24.2	0.034069	238.1	97.8	167.3	57
1.15	148	26.2	0.036942	275.4	107.1	184.7	42
1.2	166	27.3	0.038378	335.4	114.4	216.4	33

Table 4

Combustor temperature data with insulation thickness of 6 mm

Reactant Flow Rate (U): 26.09 (cm/s)							
Q _{fuel}	Q _{air}	ϕ	T1	T2	T3	Flame Speed	
1	143	1.0650	329.4	96.6	205.1	37	
1.05	125	1.1153	363.1	74.9	184.9	26	
1.15	115	1.1658	324	57.7	142.5	19	
1.2	106	1.2671	321.1	62.5	137.2	10	
Constant Equivalent Ratio (ϕ): 1.25							
Q _{fuel}	Q _{air}	U (cm/s)	Reynolds Number	T1	T2	T3	Flame Speed
1	108	22.2	0.031196	287.5	62.5	145.8	75
1.05	127	24.2	0.034069	372.2	77.4	167.5	40
1.15	148	26.2	0.036942	420.4	82.4	177.1	20
1.2	166	27.3	0.038378	462.9	93.9	209.9	12

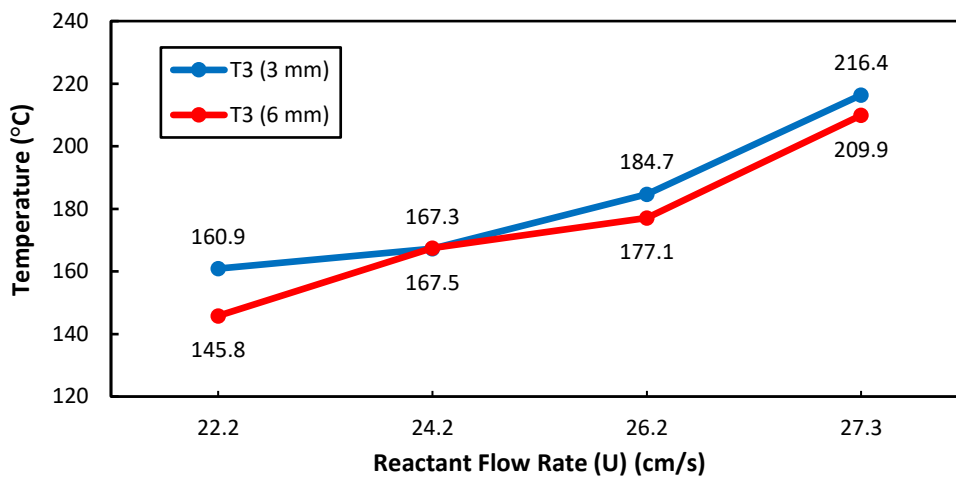


Fig. 6. Comparison of reactant flow rate with temperature distribution T3 combustor A (3 mm) and B (6 mm) in 1,25 equivalent ratios (ϕ)

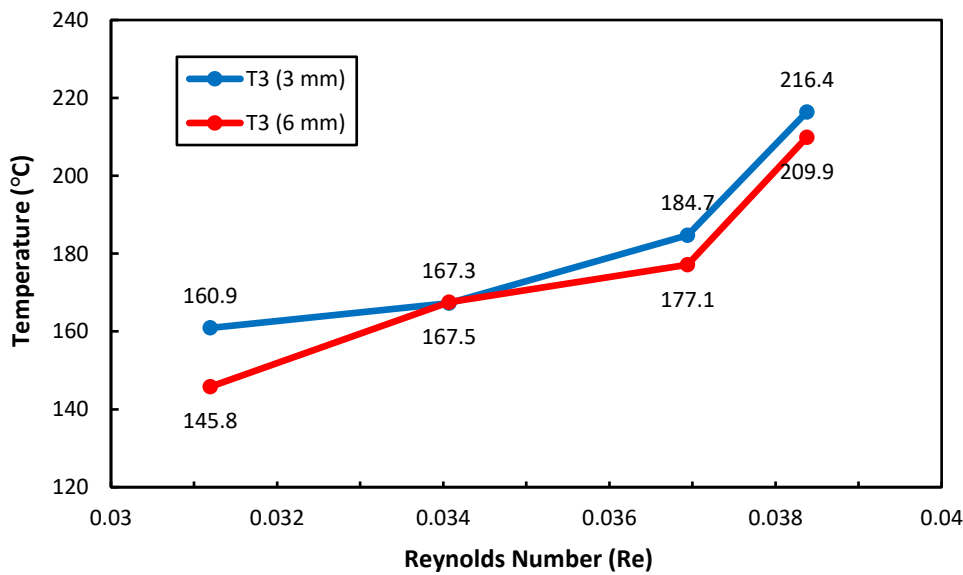


Fig. 7. Comparison of Reynolds Number with temperature distribution T3 combustor A (3 mm) and B (6 mm) in 1,25 equivalent ratios (ϕ)

In combustor A there is a regular increase in temperature along with the flow rate and Re at a constant equivalent ratio. If the air flow speed is greater, the combustion chamber temperature will be higher and the combustion rate will be faster, which will affect the fuel flow requirements in the system [20]. Combustor B has the same characteristics as combustor A. It experiences a regular increase in temperature along with the flow rate and Re at a constant equivalent ratio. This is because the higher the flow speed, the greater the air-fuel discharge. However, in increasing the temperature, combustor B is better than combustor A.

Figure 8 shows a temperature comparison with varying equivalent ratios, at a constant reactant flow rate. In combustor A, the temperature increases and decreases with increasing equivalent ratio (ϕ) as in the line pattern.

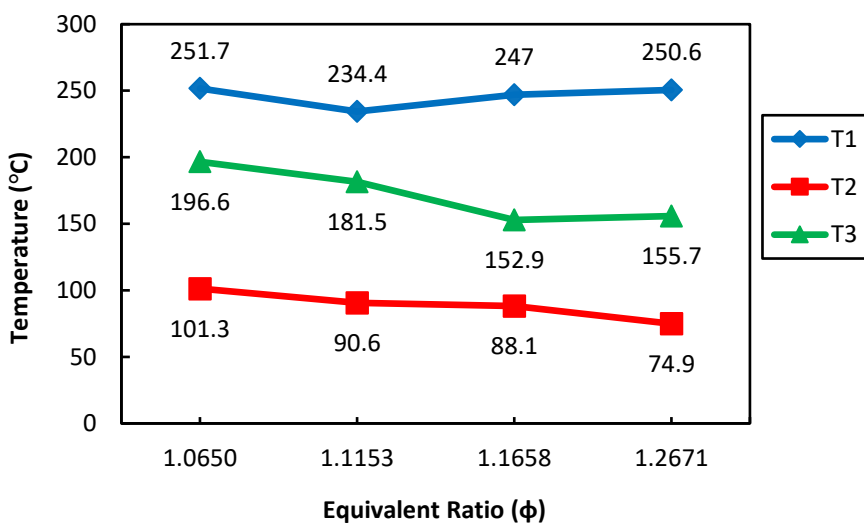


Fig. 8. Comparison of equivalent ratio with temperature distribution $T3$ of combustor A (3 mm) in a constant reactant flowrate

At a constant reactant flow rate (U), there is an increase and decrease in temperature for each addition of the equivalent ratio as shown in Figure 9. If the equivalent ratio (ϕ) is increased by adding insulation, it can reduce the heat transfer rate. Temperatures can become more stable because the insulation inhibits heat changes.

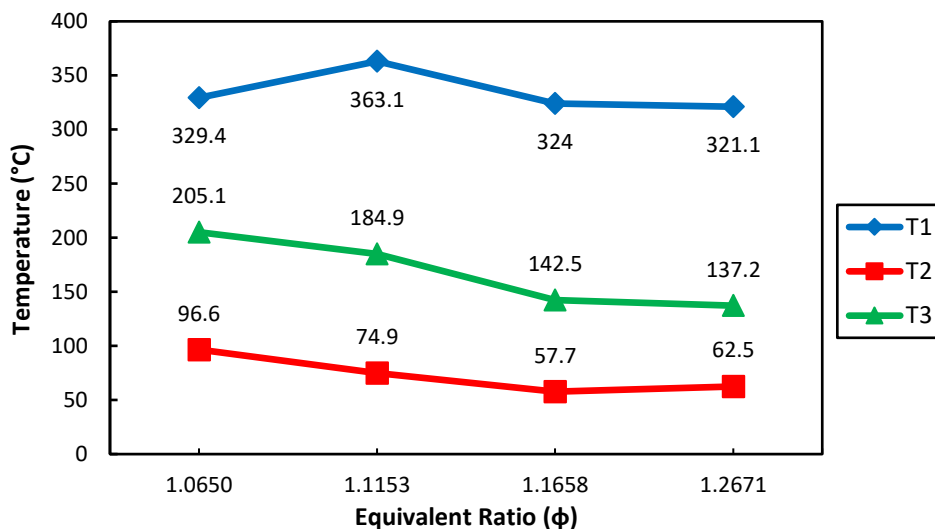


Fig. 9. Comparison of equivalent ratio with temperature distribution $T3$ of combustor B (6 mm) in a constant reactant flowrate

3.4 Heat Transfer Coefficient

The value of the convection heat transfer coefficient depends on several factors including the length of the plate through which the fluid flows, the conduction heat transfer coefficient, the speed of the fluid flow, and the kinematic viscosity of the fluid itself. The heat transfer coefficient can be found using Eq. (14).

$$\begin{aligned} \bar{h} &= 0.664 \times \frac{k}{L} Re_L^{0.5} Pr^{0.333} \quad (14) \\ &= 0.664 \times 1.4 (0.031196^{0.5})(0.674^{0.333}) \\ &= 0.014398 \text{ W/m}^2\text{C} \end{aligned}$$

3.5 Nusselt Number

Nusselt number for laminar flow in a circular pipe of diameter D with a fully developed region throughout the pipe, $Re < 2300$. The Nusselt number (Nu) on the combustor can be calculated using Eq. (15).

$$\begin{aligned} Nu &= \frac{h D}{k} \\ &= \frac{0.076946 \times 0.0095}{1.4} \\ &= 0.000522 \end{aligned} \quad (15)$$

The calculations above are plotted into a graph to make it easier to understand the graph of the Nusselt number.

The graph in Figure 10 shows that the heat transfer rate and Nusselt number with an insulation thickness of 3 mm experience a decrease and increase in the Nusselt number with each increase in heat transfer rate.

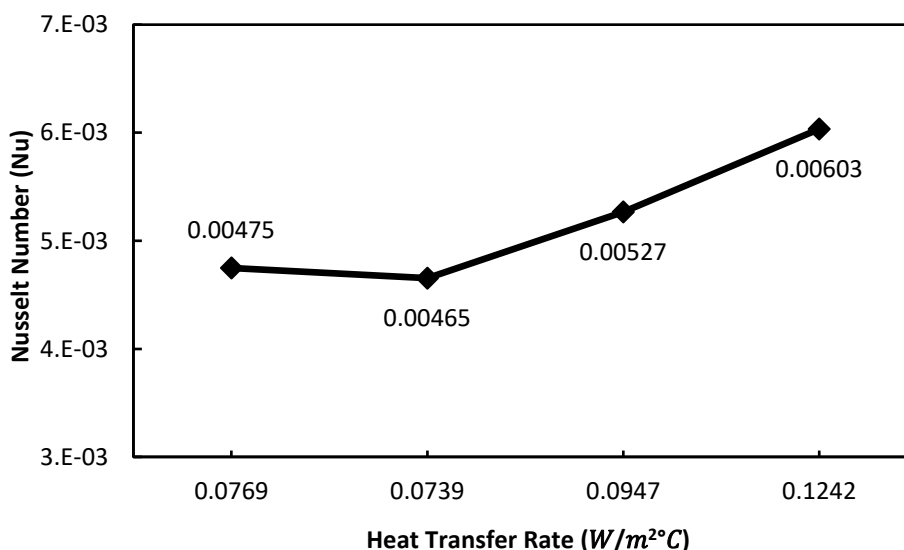


Fig. 10. Correlation between heat transfer rate and Nusselt number in 3 mm thickness with 1,25 equivalent ratios (ϕ)

The graph in Figure 11 shows that the heat transfer rate and Nusselt number with an insulation thickness of 6 mm experienced a significant increase in the Nusselt number with each additional heat transfer rate.

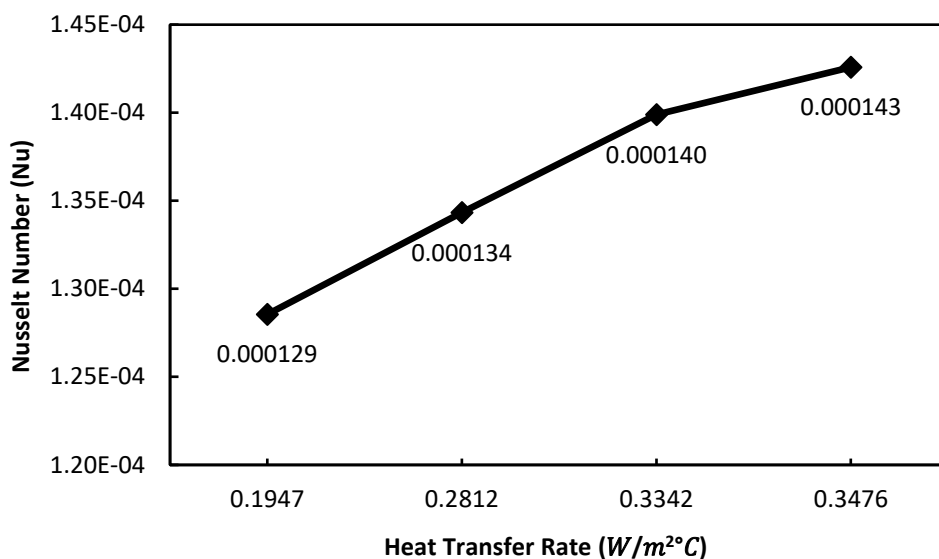


Fig. 11. Correlation between heat transfer rate and Nusselt number in 6 mm thickness with 1,25 equivalent ratios (ϕ)

3.6 Heat Transfer

After knowing the temperature T_1-T_2 in the liquid heptane fuel micro combustor, proceed to calculate the value of the heat transfer rate (qr). The tube radius (r) is 0.00475 m, length (L) 0.025 m, heat transfer coefficient (h) 1.4 W/m^2K , and temperature change (T_1-T_2) is 73.7 K. The heat transfer rate in the heptane fuel combustor can be calculated using Eq. (16).

$$qr = 2. \pi. r. L. h (T_1 - T_2) \tag{16}$$

The correlation between heat transfer rate and temperature is presented in Figure 12.

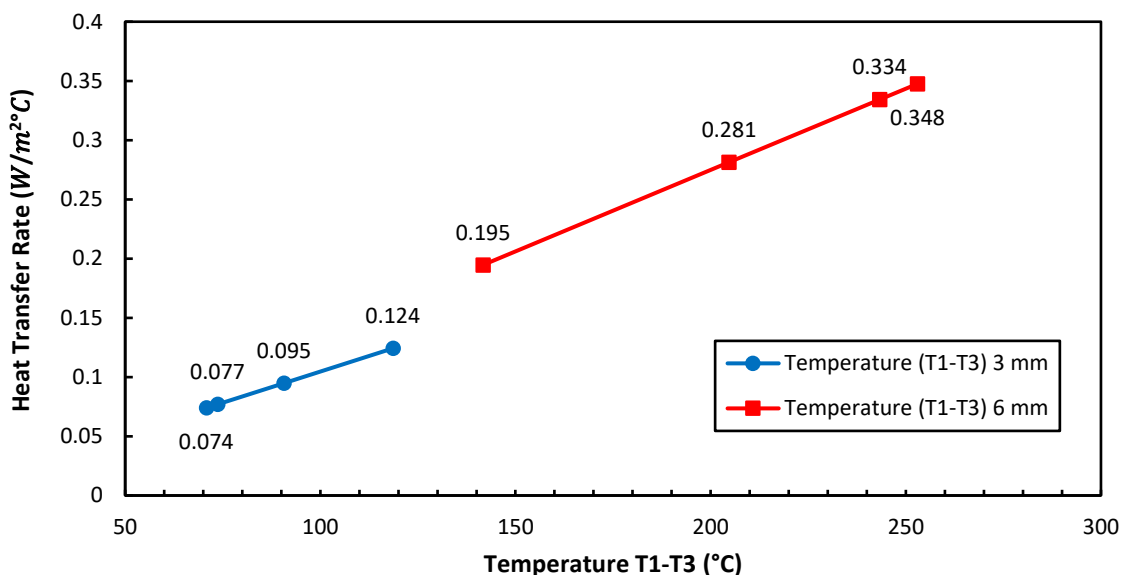


Fig. 12. Comparison of combustor A and B temperature with heat transfer rate at a constant equivalent ratio (ϕ) = 1.25

The equivalent ratio with an insulation thickness of 3 mm experiences an increase and decrease in the heat transfer rate with each increase in temperature as shown in Figure 12. The graph appears to increase and then decrease, this is caused by the thickness of the insulator which can affect the heat transfer. If the glue is thick or the insulation is thin, heat can more easily pass through the material. Thus, the temperature can rise or fall more quickly due to the lack of resistance to heat transfer.

Meanwhile, at the flow velocity and equivalent ratio with an insulation thickness of 6 mm, there is an increase in the heat transfer rate with each increase in temperature. The graph appears to be increasing steadily without any decrease, this is because the thickness of the insulating glue can affect the heat transfer. The thicker the insulating glue, the more heat it absorbs so that more temperature is stored in the insulating glue, which makes the heat transfer rate increase gradually.

This 5 mm combustor research has varying insulation thicknesses, namely 3 mm and 6 mm. When burning a thickness of 6 mm, the temperature is higher inside the combustion chamber and lower outside the combustion chamber. Adding thicker insulation can reduce heat loss because the insulation can inhibit heat transfer from the combustion chamber to the surrounding environment. Compared to the previous thickness, the 3 mm thickness has a lower temperature inside the combustion chamber and a higher temperature outside the combustion chamber. This can cause the temperature distribution at points $T1-T3$ on a 5 mm combustor with a thickness of 3 mm to have a higher temperature on the outside compared to one with a thickness of 6 mm. Meanwhile, for indoor temperatures, a combustor with a thickness of 6 mm is superior to one with a thickness of 3 mm. This is because the thickness of the insulation on the combustor can affect the temperature inside and outside the combustion chamber.

The heat transfer rate for a combustor of 5 mm with an insulation thickness of 6 mm is better than with an insulation thickness of 3 mm. This is because the heat capacity stored in an insulating glue thickness of 6 mm is greater than with a thickness of 3 mm. The flame is very sensitive to room temperature and wind in the room. A combustor with a greater thickness of insulating glue allows more heat to be absorbed and can maintain better flame stability. Meanwhile, in a combustor with a smaller thickness of insulating glue, heat will be absorbed more quickly in the insulating glue and spread more quickly at room temperature. This can cause the temperature distribution of the heat

transfer rate in a combustor with a thickness of 6 mm to be better than a combustor with a thickness of 3 mm.

4. Conclusions

The flame limit of the combustor with a mesh distance of 5 mm for liquid heptane fuel was successfully stable at an equivalence ratio 0.97–1.5 with a maximum speed of 31.7. The temperature distribution in the combustor with a mesh distance of 5 mm with an insulation thickness of 3 mm and 6 mm has its own advantages and disadvantages. The insulation thickness of 3 mm has a higher temperature on the outside and a lower temperature inside the room. Meanwhile, the insulation thickness of 6 mm has a higher temperature inside the combustion chamber and a lower temperature outside the combustion chamber.

For the heat transfer rate in the combustor, a mesh distance of 5 mm with an insulation thickness of 6 mm is better than an insulation thickness of 3 mm. This is because the heat capacity stored in an insulating glue thickness of 6 mm is greater than with a thickness of 3 mm. The next challenge in researching insulator thickness in micro combustors is the critical insulation thickness.

Acknowledgement

This research was funded by a grant from University of Muhammadiyah Malang, Indonesia.

References

- [1] Ju, Yiguang, and Kaoru Maruta. "Microscale combustion: Technology development and fundamental research." *Progress in Energy and Combustion Science* 37, no. 6 (2011): 669-715. <https://doi.org/10.1016/j.pecs.2011.03.001>
- [2] Chou, S. K., W. M. Yang, K. J. Chua, J. Li, and K. L. Zhang. "Development of micro power generators-a review." *Applied Energy* 88, no. 1 (2011): 1-16. <https://doi.org/10.1016/j.apenergy.2010.07.010>
- [3] Aravind, B., Bhupendra Khandelwal, and Sudarshan Kumar. "Experimental investigations on a new high intensity dual microcombustor based thermoelectric micropower generator." *Applied Energy* 228 (2018): 1173-1181. <https://doi.org/10.1016/j.apenergy.2018.07.022>
- [4] Munir, Fudhail Abdul, Muhmmad Ikhwan Muazzam, Abdel Gader, Masato Mikami, Herman Saputro, and Laila Fitriana. "Effects of wall thickness on flame stabilization limits for combustors with wire mesh." *Journal of Advanced Research in Fluid Mechanics and Thermal Sciences* 49, no. 1 (2018): 11-17.
- [5] Adiwidodo, Satworo, I. Nyoman Gede Wardana, Lilis Yuliati, and Mega Nur Sasongko. "Performance of cylindrical and planar mesoscale combustor with double narrow slit flame holder for micropower generator." *Eastern-European Journal of Enterprise Technologies* 2, no. 8 (2020): 104. <https://doi.org/10.15587/1729-4061.2020.198570>
- [6] Maruta, Kaoru. "Micro and mesoscale combustion." *Proceedings of the Combustion Institute* 33, no. 1 (2011): 125-150. <https://doi.org/10.1016/j.proci.2010.09.005>
- [7] Li, Guoneng, Youqu Zheng, Wenwen Guo, Dongya Zhu, and Yuanjun Tang. "Mesoscale combustor-powered thermoelectric generator: Experimental optimization and evaluation metrics." *Applied Energy* 272 (2020): 115234. <https://doi.org/10.1016/j.apenergy.2020.115234>
- [8] Yu, Xiao, Navjot S. Sandhu, Zhenyi Yang, and Ming Zheng. "Suitability of energy sources for automotive application-A review." *Applied Energy* 271 (2020): 115169. <https://doi.org/10.1016/j.apenergy.2020.115169>
- [9] Kafetzis, Alexandros, Chrysovalantou Ziogou, Simira Papadopoulou, Spyridon Voutetakis, and Panos Seferlis. "Nonlinear Model Predictive Control of an Autonomous Power System Based on Hydrocarbon Reforming and High Temperature Fuel Cell." *Energies* 14, no. 5 (2021): 1371. <https://doi.org/10.3390/en14051371>
- [10] Wan, Jianlong, and Aiwu Fan. "Recent progress in flame stabilization technologies for combustion-based micro energy and power systems." *Fuel* 286 (2021): 119391. <https://doi.org/10.1016/j.fuel.2020.119391>
- [11] Soegiharto, A. F. Hery, I. N. G. Wardana, L. Yuliati, and M. Nur Sasongko. "The use of heat circulator for flammability in mesoscale combustor." *Восточно-Европейский журнал передовых технологий* 2, no. 8 (2019): 46-56. <https://doi.org/10.15587/1729-4061.2019.155347>
- [12] Wan, Jianlong, Zuwei Xu, and Haibo Zhao. "Methane/air premixed flame topology structure in a mesoscale combustor with a plate flame holder and preheating channels." *Energy* 165 (2018): 802-811.

- <https://doi.org/10.1016/j.energy.2018.09.172>
- [13] Kusumaningsih, Haslinda, Lilis Yuliati, Rudianto Raharjo, and Ragang Aji Wibowo. "The Effect of The Inlet Reactant Direction on Circular Disk Combustor Characteristics." In *IOP Conference Series: Materials Science and Engineering*, vol. 494, no. 1, p. 012051. IOP Publishing, 2019. <https://doi.org/10.1088/1757-899X/494/1/012051>
- [14] Yuliati, Lilis. "Flame Stability of Gaseous Fuel Combustion Inside Meso-Scale Combustor with Double Wire Mesh." *Applied Mechanics and Materials* 664 (2014): 231-235. <https://doi.org/10.4028/www.scientific.net/AMM.664.231>
- [15] Bani, Stephen, Jianfeng Pan, Aikun Tang, Qingbo Lu, and Yi Zhang. "Micro combustion in a porous media for thermophotovoltaic power generation." *Applied Thermal Engineering* 129 (2018): 596-605. <https://doi.org/10.1016/j.applthermaleng.2017.10.024>
- [16] Yamamoto, Akira, Hiroshi Oshibe, Hisashi Nakamura, Takuya Tezuka, Susumu Hasegawa, and Kaoru Maruta. "Stabilized three-stage oxidation of gaseous n-heptane/air mixture in a micro flow reactor with a controlled temperature profile." *Proceedings of the Combustion Institute* 33, no. 2 (2011): 3259-3266. <https://doi.org/10.1016/j.proci.2010.05.004>
- [17] Chen, Xinjian, Junwei Li, Mang Feng, Dan Zhao, Baolu Shi, and Ningfei Wang. "Flame stability and combustion characteristics of liquid fuel in a meso-scale burner with porous media." *Fuel* 251 (2019): 249-259. <https://doi.org/10.1016/j.fuel.2019.04.011>
- [18] Salleh, Hamidon, Amir Khalid, Syabillah Sulaiman, Bukhari Manshoor, Izzuddin Zaman, Shahrin Hisham Amirnordin, Amirul Asyraf, and Wahid Razzaly. "Effects of fluid flow characteristics and heat transfer of integrated impingement cooling structure for micro gas turbine." *CFD Letters* 12, no. 9 (2020): 104-115. <https://doi.org/10.37934/cfdl.12.9.104115>
- [19] Satmoko, Ari, Engkos Achmad Kosasih, Muhammad Irfan Dzaky, Hairul Abral, Anhar Riza Antariksawan, and Andril Arafat. "Application of the Conjugate Gradient Method for Predicting Unknown Heat Flux in 2D Plat under Effect of Insulation." *Journal of Advanced Research in Fluid Mechanics and Thermal Sciences* 110, no. 2 (2023): 176-191. <https://doi.org/10.37934/arfmts.110.2.176191>
- [20] Li, Zhishuang, Ziman Wang, Haoyang Mo, and Han Wu. "Effect of the air flow on the combustion process and preheating effect of the intake manifold burner." *Energies* 15, no. 9 (2022): 3260. <https://doi.org/10.3390/en15093260>